Research article

Journal of RAMAN SPECTROSCOPY

Received: 7 June 2016 Revised: 3 August 2016 Accepted: 22 August 2016 Published online in Wiley Online Library

(wileyonlinelibrary.com) DOI 10.1002/jrs.5033

Structural characterization of phosphatidylglycerol model membranes containing the antibiotic target lipid II molecule: a Raman microspectroscopy study

M. C. Sosa Morales and R. M. S. Álvarez*

Effects induced by the incorporation of lipid II (LII) molecule into phosphatidylglycerol (PG) membranes were studied by Raman microspectroscopy. Spectral behavior of multilayer vesicles in liquid crystalline and gel phases formed by pure PG lipids and by PG/LII mixtures was evaluated. Differences shown by specific spectral markers of the lipid structure were associated with perturbations on the bilayer as response to the LII incorporation. Identification and interpretation of bands assigned to vibrations belonging to groups of the lipid polar region were supported by computational predictions. Quantum-chemical calculations – B3LYP/6-311++G(d,p) – were performed for a model charged molecule that mimics the PG lipid moiety in solvated state. Our Raman spectra demonstrate that the lipid phase is a determinant factor for both the bactoprenol tail penetration into the hydrophobic bilayer region and the perturbation degree at the membrane surface by the peptidoglycan moiety, because differential effects were observed for the two lipid systems studied. LII was able to penetrate the hydrophobic region of the lipid bilayer in the fluid phase, reaching the deep core and causing significant alterations in both the carbohydrate chain and the headgroup regions. By contrast, penetration of LII into a bilayer in the gel estate was restricted because of the high lipid packing that characterizes this phase. In this last case, interactions at the membrane surface were also indicative of partial interdigitating effect. Findings presented here provide valuable experimental evidence that contributes to the understanding of the mechanism by which lantibiotics recognize bacterial membranes. Copyright © 2016 John Wiley & Sons, Ltd.

Keywords: Lipid II; Membrane; Raman

Introduction

Understanding of structural and dynamic characteristics of biomembranes is a topic of great interest for biochemistry because one of its main goals is to explain the myriad of biochemical processes occurring in these systems.[1–3] Among them, of particular relevance are the studies regarding to the ability of some membrane-active compounds, such as antimicrobial peptides, to perturb the bacterial membranes. The membrane-active peptides can exert their activity in a direct way[4,5] and/or mediated by receptors located at the bacterial cytoplasmic membrane.[6,7] Lipid II (LII) is one of the most important receptors despite being a minor component of the bacterial membrane (less than 1 mol % of membrane phospholipids).[8] On the other hand, LII is a central component of the enzymatic cell wall building machinery because it is in charge of the translocation of monomeric peptidoglycan units from the cytoplasm to the outside of the membrane.[9]

LII consists of a long undecaprenyl (bactoprenol) hydrocarbon chain coupled to a monomeric peptidoglycan unit – the cell wall 'building block' – through a pyrophosphate linker. This block comprises two amino sugars, N-acetylglucosamine (GlcNAc) and N-acetylmuramic acid (MurNAc), with a pentapeptide bound to the latter[10] (Fig. 1).

Then, the relevance of this molecule is not only because of its function regarding the fast growing of bacterial cell wall, but also because of its structure that makes it a primary molecular target for a large number of antibiotics.[11] Specifically, some lantibiotics – a class of peptide antibiotic containing methyllantionine and some unsaturated amino acids – recognize the pyrophosphate group of LII and may interact with it by forming a kind of 'cage' with the lanthionine rings; such is the case of nisin,[12] a well-known antimicrobial peptide that is synthesized naturally by lactic acid bacteria.[13] The binding of nisin to LII causes cell lysis by membrane permeabilization and cell wall synthesis inhibition in Gram (+) and Gram (−) bacteria.[14] This interaction has been extensively studied with the aim of reaching an understanding at the molecular level of bactericidal activity of nisin, suitable to be applied to the

* Correspondence to: R. M. S. Álvarez, Instituto de Química del Noroeste Argentino (INQUINOA), Universidad Nacional de Tucumán, CONICET, Calle Batalla de Ayacucho 491, 4000 San Miguel de Tucumán, Tucumán, Argentina
E-mail: mysuko@fbqf.unt.edu.ar

Instituto de Química del Noroeste Argentino (INQUINOA), Universidad Nacional de Tucumán, CONICET, San Miguel de Tucumán, Argentina

Abbreviations: *DLPG, dilauroylphosphatidylglycerol; DPPG, dipalmitoylphosphatidylglycerol; LII, lipid II; DLPC, dilauroylphosphatidylcholine; DPPC, dipalmitoylphosphatidylcholine; PG, phosphatidylglycerol; PC, phatidylcholine; MD, molecular dynamic*

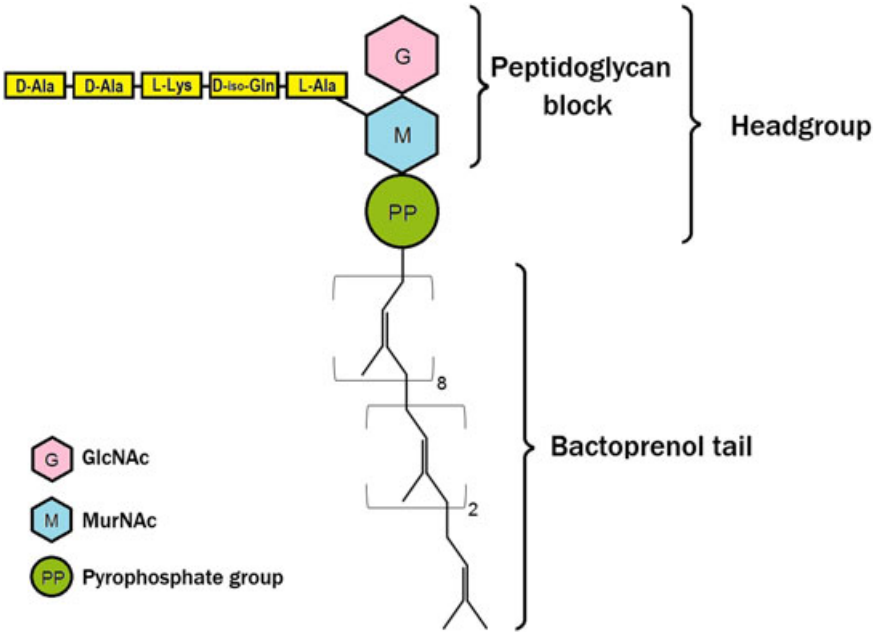

Figure 1. Schematic representation of lipid II molecule. N-acetylated sugars MurNAc and GlcNAc are shown as hexagons with M and G, respectively. The pentapeptide chain is attached to the MurNAc. The pyrophosphate moiety is shown as a circle. The bactoprenol tail is shown in abbreviated form. Pyrophosphate moiety links the peptidoglycan 'building block' to the hydrophobic prenyl chain.

development of new antibiotics.[15–19] On the other hand, a recent computational study of LII in anionic simulated membranes revealed the formation of an 'amphiphilic pattern' around the LII headgroup on the bilayer surface because of the insertion of the bactoprenol tail into the hydrophobic membrane region, and suggested the importance of this pattern in the recognition process of LII receptor by antibiotics.[20] To obtain a complete picture of these phenomena, it is essential to rely on experimental tools to provide additional structural and mechanistic information. Raman microspectroscopy (RMS) can contribute to this goal by providing solid knowledge of the interaction of LII receptor with bacterial membranes.

It is well known that Raman spectroscopy is useful to describe the changes that model membranes experience by the action of different biomolecules.[21–25] By monitoring specific bands known as sensors of the lipid packing, the number of gauche conformers in the hydrocarbon chains, and the degree of hydration of the polar headgroups, it is possible to determinate how biomolecules alter bilayer structure.[26–34]

In this paper, we study the interaction of LII with phospholipid multilayer vesicles in different lipid phases by using RMS. Taking into account that (1) the negatively charged phosphatidylglycerol (PG) lipids represent the most abundant components of bacterial membranes;[35] (2) although the liquid-crystalline (L_α) phase is the biologically most relevant membrane state, biophysical studies have shown that gel (L_β') phase plays an important role in bacterial membranes when interacts with antimicrobial peptides;[36,37] and (3) the induction of interdigitated phases in PG membranes is of high relevance to interaction studies with antimicrobial peptides because it provides a mechanism for the discrimination of membranes composed of different lipids species,[36–39] we identified and characterized structural alterations in dilauroylphosphatidylglycerol (DLPG) and dipalmitoylphosphatidylglycerol (DPPG) membrane models induced by the presence of low concentrations of LII.

Experimental

Sample preparation

DPPG and DLPG were obtained from Avanti Polar Lipids and used without further purification. Lipid II was synthesized and purified as described.[14,40] Appropriate amounts of lipids and Lipid II mixtures were dissolved in chloroform–methanol (2:1) and dried as a thin film under a nitrogen steam. Then, the samples were re-suspended by vortexing in tridistilled water at room temperature to give a final molar relation of 20:1 (lipid:LII). Although the systems thus prepared are very different from the true bacterial membranes, they represent a valuable model for the study of interactions at a molecular level between phospholipids and LII. The molar ratio here employed ensures that the effect of LII on the membrane structure is detected by Raman spectroscopy while its concentration remains relatively low.[14] Freshly prepared multilayer vesicles of DLPG and DPPG in pure state and DLPG/LII and DPPG/LII mixtures were used for Raman measurements.

Raman microspectroscopy measurements

Raman spectra between 3500 and 50 cm^{-1} were collected using a DXR Raman Microscope (Thermo Fisher Scientific). Data were collected using a diode-pump, solid state laser of 532 nm at 10 mW of power (5 cm^{-1} spectral resolution). A confocal aperture of 50-μm slit was used. Samples were focused with a 10× objective. A single drop of each sample solution was placed on gold-coated sample slides. In order to achieve a sufficient signal-to-noise ratio, spectra were collected from each vesicle by accumulating 300 spectra with an exposure time of 4 s each one. The Raman spectrum of the pure LII in solid state was also acquired. All spectroscopic experiments were carried out at ambient temperature.

Data analysis

All spectral data were processed with the OMNIC 8.3.103 Software suite (Thermo Fisher Scientific Inc.). A total number of six spectra was collected for each sample (DLPG, DLPG/LII, DPPG, and DPPG/LII), which were individually baseline corrected. A single, average spectrum was then generated for each system by taking the arithmetic mean of the corresponding six spectra. In order to compare the spectrum of pure membrane with that of the interacting membrane, the spectral contribution of the LII was subtracted from the DLPG/LII and DPPG/LII mixtures; the disappearance of the strong band at 1666 cm^{-1}, characteristic of the LII molecule,[41] was considered for the obtaining of the difference-spectra. The truncated spectral region comprised between 3100 and 900 cm^{-1} was used for the analysis.

In order to perform a detailed evaluation of the changes induced by LII in the lipid multilayer membrane, the precise position and relative intensities of the overlapping components in specific spectral regions were mathematically decomposed using the GRAMS/AI 8.0 Spectroscopy Software (Thermo Electron Corporation). The fitting result obtained using Voigt functions (that combine Gaussian and Lorentzian characters allowing each portion to have different line width)[42] was visually evaluated by overlapping the reconstituted overall curve on the original spectrum. Wavenumbers of the decomposed bands were compared with previous results obtained for the dilauroylphosphatidylcholine (DLPC) and dipalmitoylphosphatidylcholine (DPPC) lipid systems that have a zwitterionic headgroup but the same acyl chain lengths than the systems presented in this work.[23,24]

Computational calculations

Quantum-chemical calculations were performed with the Gaussian (R)03 ProgramPackage.[43] Density functional theory (DFT) calculations were carried out with the B3LYP hybrid functional.[44–46] The standard split valence basis set 6-311 ++G(d,p) was used.[47,48] In order to represent the polar headgroup of the PG lipids, the charged model system $[CH_3—O—P(O)_2—O—CH_2—CHOH—CH_2OH]^-$ was built by using the GaussView 5.0 graphical interface.[49] Geometry optimizations for different isolated conformers in vacuum were performed. The subsequent wavenumber calculation, performed at the same level of theory, allowed to ensure that the structures were true minima (imaginary wavenumbers were not obtained) and to determine the corresponding zero-point vibrational energies (ZPVEs). Latter, hydrogen-bonded dimers and trimers composed by one of the optimized conformers and one or two water molecules in different positions/orientations with respect to the P=O bonds were also optimized, and their vibrational wavenumbers were calculated.

Results and discussion

The analysis of the structural changes induced by LII in phospholipid bilayers was performed by comparing the Raman spectra of multilayer liposomes formed by pure lipids supplemented with LII. Because the main transition temperatures (T_m) for DPPG and DLPG lipids are 41 °C and −5 °C, respectively,[50] at room temperature (20 °C) the pure DLPG and DLPG/LII systems were in the liquid crystalline phase (L_α) while lipids in DPPG and DPPG/LII vesicles were in the ordered phase ($L_{\beta'}$). Figure 2 shows the spectral region comprised between 3100 and 1000 cm^{-1} of these four systems.

The evaluation of wavenumbers, relative intensities, and band shapes of specific Raman bands that account for the acyl chain conformational order, chain coupling, intramolecular motion, and relative population of *gauche* and trans conformers[26–29,31,33,34,51–53] allowed to confirm that the pure DLPG and DPPG vesicles were in the L_α and $L_{\beta'}$ states, respectively, at the experimental conditions used here. Incorporation of LII to the lipid media was manifested by subtle spectral changes in the DLPG/LII and DPPG/LII complexes with respect to the corresponding pure lipid spectra. These changes, related to structural modifications in the bilayers, are analyzed in detail. The Raman spectrum of pure LII, also included in Fig. 2, was subtracted from the DLPG/LII and DPPG/LII spectra in order to eliminate its spectral contribution. The resulting difference-spectra, named DLPG/LII-LII and DPPG/LII-LII, were acquired in base of the disappearance of the band at 1666 cm^{-1}, attributed to the bactoprenol C=C stretching.[41]

Elucidation of the subtleties of bilayer structure upon the incorporation of LII was focused on the following three spectral regions: (1) between 3100 and 2800 cm^{-1}, which corresponds to the C—H stretching modes, (2) between 1780 and 1710 cm^{-1}, typically related to the C=O stretching of the glycerol backbone, and (3) between 1150 and 1000 cm^{-1}, where the bands associated to the C—C stretching of the hydrocarbon chains as well the PO_2^- symmetric stretching and the glycerol C—O stretching of the polar headgroups are observed.[23–25,29,31,33,34]

C—H stretching modes in the acyl chains

These vibrations appear as the strongest bands of the spectra. Figure 3 shows a direct comparison between the pure PG spectra and the corresponding difference-spectra in the 3100–2800 cm^{-1} region.

All the spectra show the methylene symmetric and asymmetric stretching modes (υ_sCH_2 and $\upsilon_{as}CH_2$) at about 2850 and 2880 cm^{-1}, respectively. The ratio between their intensities, $I[\upsilon_{as}CH_2]/I[\upsilon_sCH_2]$ has been largely considered as indicative of the conformational order and lateral packing density of the acyl chains.[24,26,29,33,54] At higher wavenumbers (~2930 cm^{-1}), the Fermi resonant component of the terminal methyl symmetric stretching (υ_sCH_3) is observed; the intensity of this band shows a strong dependency of the acyl chain disorder.[28,29,31,33] In addition, the intensity ratio of υ_sCH_3 to υ_sCH_2 is commonly used as indicator of the vibrational and rotational freedom of the terminal CH_3 groups of the hydrocarbon chains; thus, the $I[\upsilon_sCH_3]/I[\upsilon_sCH_2]$ ratio increases as the inter-chain interactions decrease.[27,29,33,54]

The difference-spectrum of the fluid phase (Fig. 3a) shows a decrease of about 5% in the $I[\upsilon_{as}CH_2]/I[\upsilon_sCH_2]$ peak ratio, indicative of a decreasing in the acyl packing upon LII incorporation. Although this is not a dramatic change, it is in line with the subtle upshift of the $\upsilon_{as}CH_2$ band that points out a lowered inter-chain coupling. Furthermore, the increased $I[\upsilon_sCH_3]/I[\upsilon_sCH_2]$ ratio indicates a greater rotational freedom of the terminal CH_3 groups. Then, the observed behavior of the C—H stretching bands suggests that the LII is able to penetrate deep inside the bilayer in the L_α state. A recent study of the conformational properties of LII in bacterial membranes by molecular dynamic (MD) simulations has shown that the long bactoprenol tail of LII can penetrate the hydrophobic membrane region and adopts different conformations, being the most typical that with the terminal part

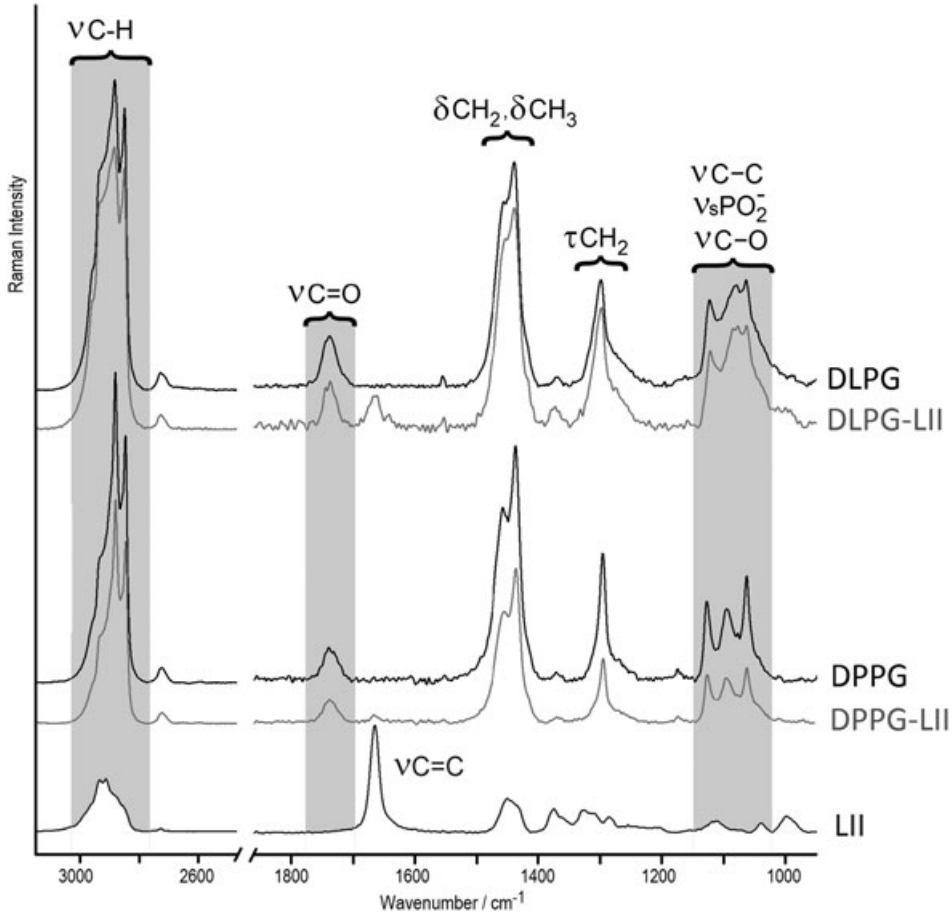

Figure 2. Raman spectral regions in the 3100–2700 and 1800–800 cm^{-1} intervals of multilamellar vesicles of DLPG and DPPG in pure state and DLPG/LII and DPPG/LII mixtures. Sample measurements were performed at room temperature. Band assignment of the main lipid vibrations is included. Specific bands considered in this analysis appear highlighted by shaded areas. Raman spectrum of LII in pure state is also shown.

of the tail residing between two monolayers.[20] This simulated behavior of LII in a fluid lipid membrane supports our spectral observations.

The effect of LII incorporation to membranes in the gel state appears less pronounced than in the liquid crystalline phase because only a decrease of about 3% in the $I[\upsilon_{as}CH_2]/I[\upsilon_sCH_2]$ ratio is estimated (see Fig. 3b). Moreover, the rotational CH_3 motions result more restricted in comparison with that in pure DPPG vesicles – the $I[\upsilon_sCH_3]/I[\upsilon_sCH_2]$ ratio decreases 4% approximately with the presence of LII. The characteristic high lipid packing of the gel phase is the responsible of the reduced penetration of LII. The spectral behavior of the C—H stretching bands suggests that LII is unable of reaching the deep core of the DPPG membrane; in its instead partial interdigitation in the lipid bilayer is induced, as is derived from the reduced freedom of the terminal CH_3 groups of the acyl chains. The tendency of some amphiphilic, bulky membrane-active compounds to induce hydrocarbon chain interdigitation has been well demonstrated; these biomolecules, by acting preferentially near the lipid polar interface, affect the balance between the headgroup and chain interactions and form the interdigitated phase.[36,38,39] The limited penetration of LII into the DPPG membrane may modify the lateral stress profile at the water/bilayer interfacial region and induced partial interdigitation. Further evidences of this effect will be discussed below.

C—C stretching modes in the acyl chains

The spectral region comprised between 1150 and 1000 cm^{-1} of the DLPG and DPPG containing systems is shown in Figures 4 and 5, respectively.

Valuable information can be extracted from this region because several prominent bands, originated by the methylene C—C stretching modes, are observed. The relevance of these bands is based on the fact that they directly reflect intramolecular trans–*gauche* conformational changes within the hydrocarbon chains region of the lipid matrix.[29,33,54] In addition, the symmetric stretching of the PO_2^- groups ($\upsilon_sPO_2^-$) and the stretching of the glycerol C—O bonds (υC—O) of the lipid polar heads are also expected around 1000–1100 cm^{-1} in the membrane Raman spectra.[23–25,31] Band decomposition by applying a curve fitting procedure was required to perform a detailed analysis of this highly complex spectral region. Typically, the Raman spectra of the four studied systems show two sharp bands at ~1124–1128 cm^{-1} and ~1063 cm^{-1} which are straightforward assigned to the in phase and out-of-phase C—C stretching modes of trans conformers ($\upsilon_{i.ph.}(C—C)_T$ and $\upsilon_{o.o.ph}(C—C)_T$, respectively).[29,31,33] The spectral profile delimited by these two strong bands characterizes the lipid disorder because it contains the bands corresponding to C—C stretching modes of *gauche* defects in the acyl chains. Because these defects can be localized at different positions along the acyl

Journal of RAMAN SPECTROSCOPY

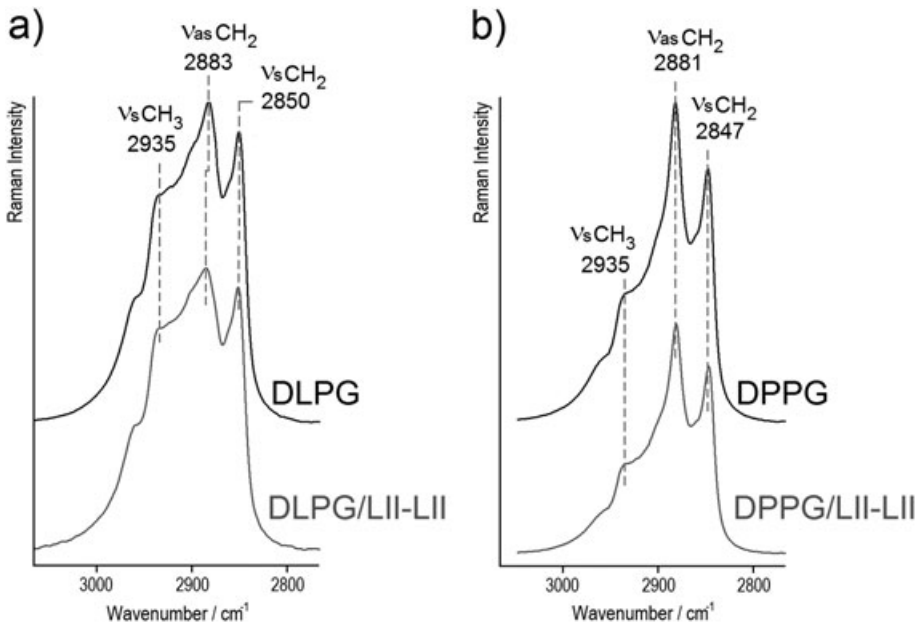

Figure 3. Spectral region corresponding to methylene and methyl C—H stretching vibrations of phospholipid acyl chains. Pure DLPG and DPPG multilamellar vesicles – a) and b), respectively – are compared with the corresponding difference-spectrum obtained by subtracting the LII spectrum from the PG/LII mixture (DLPG/LII-LII and DPPG/LII-LII).

chain, they originate different features whose intensities are strongly dependent on the lipid phase: the band at ~1084 cm^{-1}, associated to *gauche* conformers at the chain ends (end-*gauche*, $\upsilon(C—C)_{e\text{-}G}$), is observable even in the ordered phase;[33] the band at ~1077 cm^{-1}, corresponding to *gauche*–trans–*gauche* ($\upsilon(C—C)_{G\text{–}T\text{–}G}$) conformations in the body of the chain is typical for the L_α phase;[23–25,55–58] a third type of kinked-chain structure, the double-*gauche* ($\upsilon(C—C)_{G\text{-}G}$) conformation, can be also observed at ~1070 cm^{-1},[23,56] although this conformation is considerably less abundant and further studies should be perform to reach a more confident characterization. It is worth mentioning that the spectral decomposition and subsequent interpretation show consistency with previous results we obtained for DLPC and DPPC lipid membranes in pure state and in interaction with several thyroid hormones.[23–25] Structural similarities and differences among the studied systems correlate well in number, position, and relative intensities of the C—C bands attributed to *gauche* defects.

DLPG and DLPG/LII-LII Raman spectra (Fig. 4) show a complex band contour evidencing several strong components which fitted well with seven decomposed bands contained between the $\upsilon_{i.ph}(C—C)_T$ and $\upsilon_{o.o.ph}(C—C)_T$ bands. The component bands located at 1084, 1077, and 1071 cm^{-1} in DLPG are assigned to the C—C stretching of the abundant *gauche* defects that characterize the fluid lipid phase. The components at higher wavenumbers are associated with vibrations located in the polar headgroups, which will be discussed later. On the other hand, according to a conformational study for the *ortho*-phophate headgroup of phospholipids, the component at approximately 1050 cm^{-1} is assigned to the C—O stretching of the phosphate ether group; [59] this component was also observed in the Raman spectra of the PC systems.[23,24] The remaining components appearing at lower wavenumbers are not assigned; they would be attributed to vibrations involving the glycerol portion of the PG systems because they were not observed in the spectra of the phosphatidylcholine lipids.[23,24] Upon LII incorporation, a significant intensification is manifested in the band contour and, consequently, in the intensities of the decomposed bands. Semi quantitative determinations of the content of trans and *gauche* conformers in the acyl chains were performed. The intensity ratios of the bands assigned to the *gauche* conformers with respect to that corresponding to the trans conformers in out-of-phase stretching ($I\upsilon(C—C)_G/I\upsilon_{o.o.ph}(C—C)_T$) were calculated.[23,29,33] The comparison between the ratios obtained from the DLPG and DLPG/LII-LII spectra indicates that LII induces increments about 30% and 45% in the population of the end-*gauche* and *gauche*–trans–*gauche* conformers, respectively. This behavior of the C—C stretching bands, together with that observed in the region of the C—H stretching modes, suggests that LII is able of penetrating in the deep interior of the bilayer and exerts structural alteration in this region. MD simulations of LII in bacterial membranes showed that the flexible bactoprenol chain of LII explores the whole hydrophobic slab in the membrane inducing high distortions all along the lipid acyl chains; moreover, the terminal CH_3 groups of the LII tail are capable of travelling from one membrane surface to the other, although the most probable conformation is that with the final portion of the tail located between two monolayers (L-shape).[20] The increased chain disorder evidenced by the higher population of *gauche* conformers is in line with the decreased inter-chain coupling derived from the C—H stretchings; both spectral observations correlate with the results obtained by MD simulations.

The lipid systems in gel phase show a broad, medium-intensity band centered at 1095 cm^{-1} and a weak band at 1078 cm^{-1} (Fig. 5a). From the several component bands observed upon spectral decomposition, only two bands are attributed to C—C stretching of *gauche* conformers; the remaining components belong to vibrations on the polar headgroups. According to the ordered phase, the pure DPPG spectrum evidences a few end-*gauche* conformers (1086 cm^{-1}) and an even smaller proportion of isolated *gauche* defects in the body of the acyl chains (1078 cm^{-1}). The relative intensities of these two bands appear markedly altered in the DPPG/LII-LII spectrum pointing out the incorporation of LII to the bilayer induces a decrease of 20% in the population of end-*gauche*

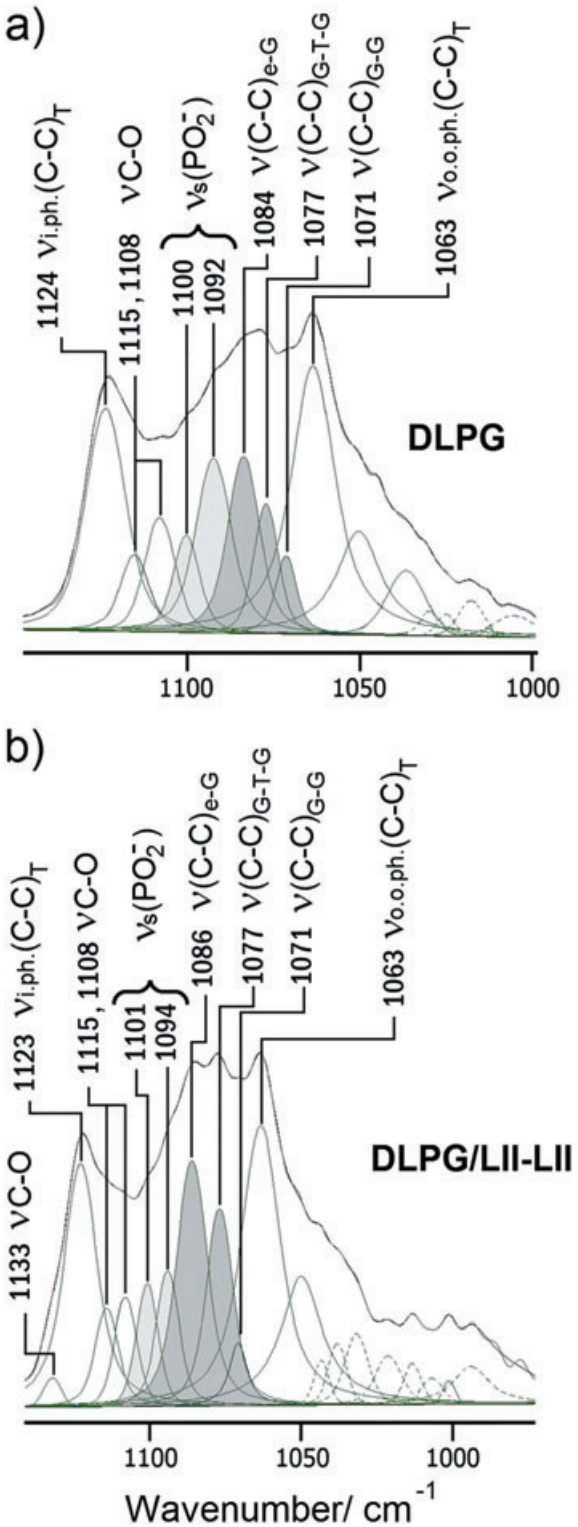

Figure 4. Spectral region corresponding to the C—C stretching vibration of the acyl chains of phospholipids in the liquid-crystalline phase. Other stretching modes belonging to the phosphate and glycerol groups of the lipid polar head are also expected in this region. The positions and relative intensities of the components contributing to the complex band profile are estimated by using a curve-fitting procedure; the reconstructed band is superimposed on the original spectrum in order to show the level of fit attained. a) pure DLPG and b) DLPG/LII-LII difference-spectrum.

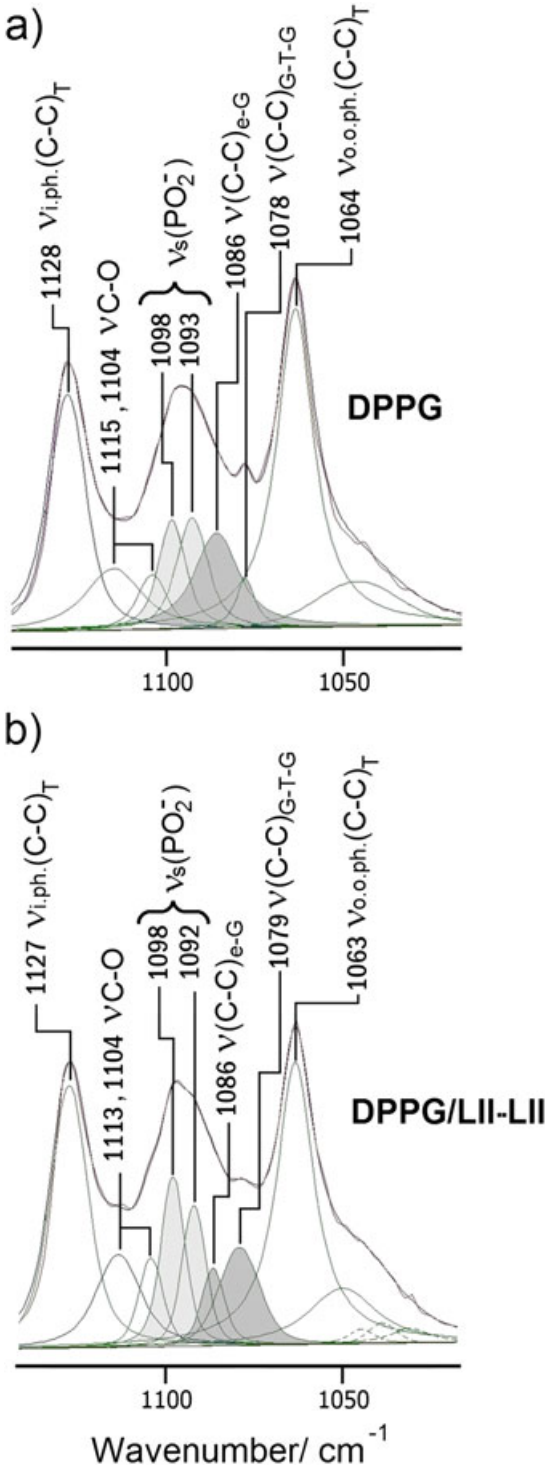

Figure 5. Spectral region corresponding to the C—C stretching vibration of the acyl chains of phospholipids in the gel phase. Other stretching modes belonging to the phosphate and glycerol groups of the lipid polar head are also expected in this region. The positions and relative intensities of the components contributing to the complex band profile are estimated by using a curve-fitting procedure; the reconstructed band is superimposed on the original spectrum in order to show the level of fit attained. a) pure DPPG and b) DPPG/LII-LII difference-spectrum.

conformers and an increment of ca. 40% in the relative number of G–T–G defects (Fig. 5b). This spectral analysis is in concordance with that derived from the evaluation of the corresponding C—H

stretching modes and confirms the assumption that LII induces partial interdigitation when interacts with a membrane in the gel state. The superficial penetration of LII tail into the hydrocarbon chains may alter the lateral stress at the interfacial region and causes this effect.[36,38,39]

Symmetric PO_2^- and C—O stretching modes in the polar headgroups

The peak fitting procedure applied to the spectral range comprised between 1000 and 1150 cm^{-1} reveals also the presence of several overlapped bands attributable to the $\upsilon_s PO_2^-$ and υC—O modes of the lipids polar headgroups (see Figs 4 and 5). The assignment of these features is based on reported experimental values for PG and PC model membranes in different phase states;[23–25,31] quantum chemical calculations for the charged molecule $[CH_3—O—P(O)_2—O—CH_2—CHOH—CH_2OH]^-$ that mimics the PG moiety; and MD simulations of pure PG membranes in liquid crystalline and gel states.[60–62] Predicted wavenumbers for the hydroxyl C—O bonds and the $\upsilon_s PO_2^-$ mode are listed in Table 1.

The bands at 1115–1108 cm^{-1} (in DLPG spectrum, Fig. 4a) and at 1115–1104 cm^{-1} (in DPPG spectrum, Fig. 5a) are associated with the C—O stretching modes belonging to the glycerol moiety. The absence of these bands in the spectra of DLPC and DPPC membranes supports this assignment.[23,24] In addition, calculations predicted the υC—O modes at higher wavenumbers than the $\upsilon_s PO_2^-$ mode for various stable conformations of the model molecule (Table 1). The bands observed at 1100 and 1092 cm^{-1} in DLPG (Fig. 4a) and at 1098 and 1093 cm^{-1} in the DPPG spectrum (Fig. 5a) are assigned to the $\upsilon_s PO_2^-$ vibration. According to the MD simulations, this charged group shows a high tendency to form intermolecular H-bond associations with water molecules and/or with glycerol OH groups of adjacent lipids in addition to the intramolecular H-bonds with glycerol hydroxyls; the presence of Na^+ ions also contributes to reduce the interlipid charge-charge repulsion.[60–62] In order to connect the structural insights provided by the MD simulations with the vibrational behavior experimentally observed by Raman spectroscopy, we performed quantum-chemical calculations for the model molecule in different conformations, both in free state and in the presence of one or two H-bonded water molecules, and with or without Na^+ ions. Our computational results show that the $\upsilon_s PO_2^-$ tends to increase the wavenumbers when is involved in intermolecular interactions while downshifts would be expected upon intramolecular associations; a compromise between both trends is observed in mixed H-bond interactions. Although the experimental evidence does not support a rigorous differentiation between intra- and intermolecular associations, we propose a detailed assignment of the bands belonging to the polar headgroups based on the computational predictions and previous studies of lipid membranes upon interaction with biomolecules.[23–25] Thus, the bands at 1100 cm^{-1} (DLPG spectrum) and at 1098 cm^{-1} (DPPG spectrum) are tentatively assigned to $\upsilon_s PO_2^-$ of intermolecular H-bonded groups, while the bands at 1092 and 1093 cm^{-1} (in DLPG and DPPG spectra, respectively) are assigned to the stretching of phosphate groups in intramolecular associations with the glycerol OH groups. Previously published, Raman spectra of DLPC and DPPC lipids showed a single band attributable to the $\upsilon_s PO_2^-$ mode (1100 cm^{-1}) because only intermolecular H-bond interactions are present in these systems.[23,24] In the DLPG/LII-LII spectrum, the component at lower wavenumbers (1094 cm^{-1}) experiences an important loss of intensity while that at 1101 cm^{-1} enhances (Fig. 4b). Based on the proposed interpretation for the $\upsilon_s PO_2^-$ bands, this behavior suggests that the insertion of LII breaks some intramolecular H-bonds, probably because of structural modifications in the interfacial region, while promotes the formation of intermolecular associations with the LII head

Table 1. Calculated wavenumbers at the B3LYP/6-311++g(d,p) level for the symmetric stretching of the phosphate ($\nu_s PO_2^-$) and the C—O stretching of the glycerol terminal (νCOH_{ter}) and intermediate (νCOH_{int}) hydroxyl groups, predicted for the charged $[CH_3—O—P(O)_2—O—CH_2—CHOH—CH_2OH]^-$ model molecule in vacuum. Optimizations for different, stable conformers in isolated state and forming dimmers and trimmers with one or two water molecules were prior calculated. A single Na^+ ion was also added. The numbers in parenthesis are used to identify the H-bonded water molecule. Although the calculated wavenumbers differ from those observed upon deconvolution of the experimental spectra (Fig. 3), the overall trend supports our spectral interpretation

$\upsilon_s PO_2^-$ (cm^{-1})	N°	Association		υC—OHint (cm^{-1})	N °	Association		υC—OHter (cm^{-1})	N °	Association	
		Type	Group			Type	Group			Type	Group
1059	—	—	—	1082	1	Intra	C—O—P	1045	1	Intra	COH int
1039	1	Intra	COH int	1148	1	Intra	P=O	1093	1	Intra	COH int
					1	Intra	COH ter				
1040	1	Intra	COH int	1126	1	Intra	P=O	1062	1	Intra	C—O—P
1045	1	Intra	COH ter	1122	1	Inter	H_2O (1)	1077	1	Intra	P=O
	1	Inter	H_2O (1)								
1061	1	Intra	COH ter	1105	1	Inter	H_2O (2)	1085	1	Intra	P=O
	2	Inter	H_2O (1)								
	1	Inter	H_2O (2)								
1070	2	Inter	H_2O (1)	1084	1	Intra	C—O—P	1050	1	Intra	COH int
1058	1	Intra	COH ter Na^+	1105	1	Intra	C—O—P	1083	1	Intra	P=O
1069	1	Inter	H_2O (1) Na^+	1129	1	Intra	C—O—P Na^+	1050	1	Intra	COH int
1070	1	Intra	COH ter	1082	1	Inter	H_2O (2)	1026	1	Intra	P=O
	1	Inter	H_2O (1)								Na^+
	1	Inter	H_2O (2) Na^+								

and/or with neighboring phospholipids. In addition, a change in the relative intensities of the glycerol υC—O bands confirms the assumption that the interactions of LII at the lipid polar interface induce structural alterations. The appearance of a weak component at 1133 cm^{-1} could be also a consequence of this perturbation; because this band is absent in the other spectra (e.g. DLPG, DPPG, and DPPG/LII-LII), we assume that LII forces to some glycerol COH groups to take part of less probably hydrogen-bonding interactions and/or different conformations (high wavenumbers were calculated for this vibration in some cases, see Table 1). MD simulations to study the dynamic properties of LII in a simulated bacterial membrane indicated the existence of (1) specific interactions between the phospholipid PO_2^- group and the positively charged lysine residue of the LII pentapeptide moiety, (2) high distortion in the surface bilayer because of the large-amplitude motions of the LII tail incorporated into the hydrophobic region, and (3) creation of amphiphilic patterns on the membrane surface consisting in a large horseshoe-shaped hydrophobic surface around the LII head with a hydrophilic area inside it.[20] Particularly, this last statement supports our interpretations.

The effect induced by LII on the polar headgroup region of the DPPG membrane is manifested by the enhancement of the band at 1098 cm^{-1} (DPPG/LII-LII spectrum, Fig. 5b) which is interpreted as an increment of intermolecular H-bond formations; the rest of features remained almost unchanged suggesting the existence of poor interactions between LII and the interfacial region of the membrane. The tight inter-lipid packing that characterizes the gel phase[62] may be responsible for this limited penetration of LII into the bilayer. However, according to the spectral evidence presented here the interactions of LII with the phosphate group of the DPPG membrane would be enough to cause interdigitation.

C=O stretching mode of the diacylglycerol backbone

Interactions at the interfacial level are evaluated in based on the C=O band that appeared around 1740 cm^{-1}. This vibration appears in the Raman spectra of lipid membranes as a weak band with complex contour because of the different conformations and hydration degree.[25,63–66] MD simulations of DOPG and DPPG bilayers in the liquid crystalline and gel phases, respectively, described different environments surrounding the ester C=O groups.[61,62] The published results for the fluid phase indicate that strong associations with Na^+ ions make water molecules squeezed out from the first coordination shell of the C=O group, while intermolecular H-bond formation with glycerol hydroxyl groups of adjacent lipids is favored by the almost parallel orientation of the headgroups to the membrane surface.[61] MD simulations of DPPG bilayer indicated a different arrangement of the lipid headgroups in this ordered system: here, the diacylglycerol backbones takes a more parallel orientation with respect to the normal to the bilayer, thus hindering any form of favorable association either with Na^+ ions, with water molecules, or with neighboring lipids. In addition, the carbonyl groups are restricted to move freely, which lowers their ability to form hydrogen bridges.[62] Both scenarios estimated by the MD simulations are manifested to some extent in our Raman spectra (Fig. 6).

The spectrum of DLPG shows a band centered at 1739 cm^{-1} with a smooth shoulder at 1744 cm^{-1}, indicating a high conformational freedom of the carbonyl groups, which are mainly participating in H-bonding associations, as is expected for the fluid phase.[25,65] On the contrary, in the DPPG spectrum, a band with maximum at 1741 cm^{-1} and several well defined shoulders at both sides are consistent with the existence of more rigid conformations of the acyl linkage in the sn_1 and sn_2 chains, with an important contribution from non-associated C=O groups.[25,64,65] In the spectrum DLPG/LII-LII, the C=O band appears narrower than in pure DLPG, and its shape resembles the profile observed for the membrane in the gel phase, suggesting the rupture of some interactions involving the carbonyl groups. This interpretation is supported by MD simulations of LII in a fluid bilayer that predicted the appearance of hydrophobic clusters on the membrane surface because of some conformations adopted by the LII tail and by the disorder of the highly perturbed phospholipid acyl chains.[20] On the other hand, the poor penetration of the LII head into the interfacial region of the membrane in gel phase is also manifested in the behavior of the carbonyl groups because relevant spectral differences are not observed between the C=O bands in the DPPG and DPPG/LII-LII spectra.

Figure 7 provides a rough visualization of the differential ability of LII to penetrate lipid membranes in different phase states as well as the main interactions and structural effects that derived from the Raman spectral analysis.

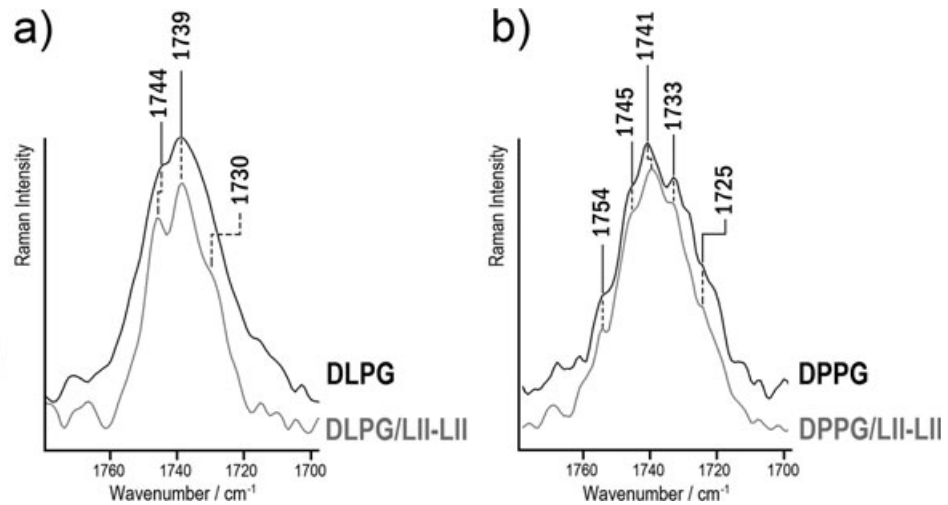

Figure 6. Raman spectra in the region corresponding to the carbonyl stretching modes of the acyl chains. Pure DLPG and DPPG multilamellar vesicles – a) and b), respectively – are compared with the corresponding difference-spectrum obtained by subtracting the LII spectrum from the PG/LII mixture (DLPG/LII-LII and DPPG/LII-LII).

Journal of RAMAN SPECTROSCOPY

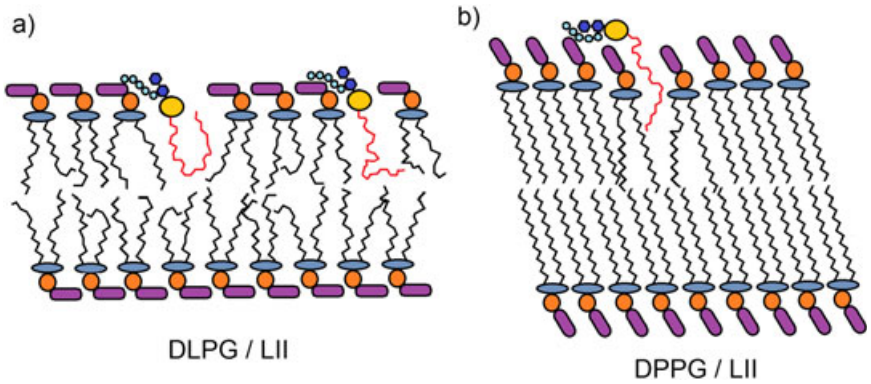

Figure 7. Schematic representation of the phospholipids/LII systems with lipids in two different phases. a) Bilayer in the liquid crystalline state containing LII molecules; two different arrangements of LII into the membrane are illustrated to show only some of the possible orientations that the bactoprenol chain can adopt when is inserted into the hydrophobic membrane region. b) Bilayer in the gel state containing LII; a partial interdigitation between the hydrocarbon chains is shown.

Conclusions

We present a Raman spectroscopy study of the effects exerted by LII in anionic membranes in two different phases. The observed spectral changes indicate that LII is able to penetrate the hydrophobic region of the lipid bilayer in the fluid phase, causing significant alterations in both the carbohydrate chain and the headgroup regions. The decreased inter-chain coupling and the increment in the population of *gauche* defects all along the acyl chains indicate that the bactoprenol chain can reach the deep core of the bilayer. Strong interactions at the membrane surface are evidenced not only by the formation of additional intermolecular H-bond associations between the pentapeptide moiety of LII and the phosphate groups of lipids but also by structural rearrangements affecting the inter/intramolecular associations among the glycerol COH, the PO_2^-, and the C=O groups, including water molecules. The incorporation of LII into a bilayer in the gel phase results markedly restricted by the high density packing that characterizes the ordered phase. Although our Raman spectra reveal only a weak effect produced by the peptidoglycan-pyrophosphate block of LII on the phospholipid headgroups, the decreased mobility at the terminal segment of the lipid chains suggests that the existence of interactions at the membrane surface is inductive of partial interdigitation in the bilayer.

The overall results here presented indicate that specific interactions between lipid II and phospholipids modulate particular bilayer conformations according to the lipid phase. These 'membrane responses' would play a key role in the bacterial membrane recognition process by lantibiotics. Further Raman studies of these LII-embedded systems in interactions with antimicrobial agents are required.

Acknowledgements

Authors thank Prof. Dr. Eefjan Breukink and his group from Utrecht University, The Netherlands, for their valuable assistance with Lipid II synthesis and purification. This work was partially supported by CONICET, National University of Tucumán, Grant PIP-CONICET 2011-0303, and Grant ANPCyT PICT 2012 N° 299 to R.M.S.A. M.C.S. M. is grateful to CONICET for a Doctoral Fellowship. R.M.S.A. is a career researcher of CONICET. All authors read and approved the final article.

References

[1] J. F. Nagle, S. Tristram-Nagle, *Biochim. Biophys. Acta* **2000**, *1469*, 159.
[2] J. Katsaras, T. Gutberlet, *Lipid Bilayers: Structure and Interactions*, Springer-Verlag, Berlin, **2001**.
[3] S. Tristram-Nagle, J. F. Nagle, *Chem. Phys. Lipids* **2004**, *127*, 3.
[4] C. van Kraaij, E. Breukink, M. A. Noordermeer, R. A. Demel, R. J. Siezen, O. P. Kuipers, B. de Kruijff, *Biochemistry* **1998**, *37*, 16033.
[5] D. Sengupta, H. Leontiadou, A. E. Mark, S. -J. Marrink, *Biochim. Biophys. Acta* **2008**, *1778*, 2308.
[6] A. Wiese, K. Brandenburg, A. J. Ulmer, U. Seydel, S. Müller-Loennies, *Biol. Chem.* **1999**, *380*, 767.
[7] E. Breukink, B. de Kruijff, *Nat. Rev. Drug Discovery* **2006**, *5*, 321.
[8] N. E. Kramer, E. J. Smid, J. Kok, B. de Kruijff, O. P. Kuipers, E. Breukink, *FEMS Microbiol. Lett.* **2004**, *239*, 157.
[9] B. de Kruijff, V. van Dam, E. Breukink, *Prostaglandins Leukot. Essent. Fatty Acids* **2008**, *79*, 117.
[10] M. S. VanNieuwenhze, S. C. Mauldin, M. Zia-Ebrahimi, B. E. Winger, W. J. Hornback, S. L. Saha, J. A. Aikins, L. C. Blaszczak, *J. Am. Chem. Soc.* **2002**, *124*, 3656.
[11] T. Schneider, H. G. Sahl, *Int. J. Med. Microbiol.* **2010**, *300*, 161.
[12] S. T. D. Hsu, E. Breukink, E. Tischenko, M. A. G. Lutters, B. de Kruijff, R. Kaptein, A. M. J. J. Bonvin, N. A. J. van Nuland, *Nat. Struct. Mol. Biol.* **2004**, *11*, 963.
[13] W. B. Buchman, S. Banerjee, J. R. Hansen, *J. Biol. Chem.* **1988**, *263*, 16260.
[14] I. Wiedemann, E. Breukink, C. van Kraaij, O. P. Kuipers, G. Bierbaum, B. de Kruijff, H. G. Sahl, *J. Biol. Chem.* **2001**, *276*, 1772.
[15] H. E. van Heusden, B. de Kruijff, E. Breukink, *Biochemistry* **2002**, *41*, 12171.
[16] E. Breukink, H. E. van Heusden, P. J. Vollmerhaus, E. Swiezewska, L. Brunner, S. Walker, A. J. R. Heck, B. de Kruijff, *J. Biol. Chem.* **2003**, *278*, 19898.
[17] I. Wiedemann, R. Benz, H. G. Sahl, *J. Bacteriol.* **2004**, *186*, 3259.
[18] H. E. Hasper, B. de Kruijff, E. Breukink, *Biochemistry* **2004**, *43*, 11567.
[19] D. C. Koch, T. H. Schmidt, H. G. Sahl, U. Kubitscheck, C. Kandt, *Biochim. Biophys. Acta* **2014**, *1838*, 3061.
[20] A. Chugunov, D. Pyrkova, D. Nolde, A. Polyansky, V. Pentkovsky, R. Efremov, *Sci. Rep.* **2013**. DOI:10.1038/srep01678.
[21] R. M. S. Alvarez, C. O. Della Védova, H. G. Mack, R. N. Farías, P. Hildebrandt, *Eur. Biophys. J.* **2002**, *31*, 448.
[22] R. M. S. Alvarez, E. H. Cutin, R. N. Farías, *J. Membr. Biol.* **2005**, *205*, 61.
[23] A. A. Petruk, R. M. S. Alvarez, *J. Raman Spectrosc.* **2013**, *44*, 346.
[24] A. A. Petruk, M. C. Sosa Morales, R. M. S. Alvarez, *Spectrochim. Acta, Part A* **2013**, *112*, 403.
[25] M. C. Sosa Morales, A. C. Juarez, R. M. S. Alvarez, *J. Raman Spectrosc.* **2015**, *46*, 302.
[26] R. G. Snyder, J. R. Scherer, B. P. Gaber, *Biochim. Biophys. Acta* **1980**, *601*, 47.
[27] R. G. Snyder, H. L. Strauss, C. A. Elliger, *J. Phys. Chem.* **1982**, *86*, 5145.
[28] F. Lhert, F. Capelle, D. Blaudez, C. Heywang, J. M. Turlet, *J. Phys. Chem. B* **2000**, *104*, 11704.
[29] C. J. Orendorff, M. W. Ducey Jr., J. E. Pemberton, *J. Phys. Chem. A* **2002**, *106*, 6991.

[30] D. P. Cherney, J. C. Conboy, J. M. Harris, *Anal. Chem.* **2003**, *75*, 6621.
[31] A. Csiszár, E. Koglin, R. J. Meier, E. Klumpp, *Chem. Phys. Lipids* **2006**, *139*, 115.
[32] A. Ianoul, H. Westwick, L. Nowacka, B. Quan, *J. Raman Spectrosc.* **2007**, *38*, 200.
[33] C. B. Fox, R. H. Uibel, J. M. Harris, *J. Phys. Chem. B* **2007**, *111*, 11428.
[34] C. B. Fox, J. M. Harris, *J. Raman Spectrosc.* **2010**, *41*, 498.
[35] 35. F. Prossnigg, A. Hickel, G. Pabst, K. Lohner, *Biophys. Chem.* **2010**, *150*, 129.
[36] G. Pabst, S. Danner, S. Karmakar, G. Deutsch, V. A. Raghunathan, *Biophys. J.* **2007**, *93*, 513.
[37] E. Sevcsik, G. Pabst, A. Jilek, K. Lohner, *Biochim. Biophys. Acta* **2007**, *1768*, 2586.
[38] T. Mavromoustakos, P. Chatzigeorgiou, C. Koukoulitsa, S. Durdagi, *Int. J. Quantum Chem.* **2011**, *111*, 1172.
[39] T. Mavromoustakos, P. Moutevelis-Minakakis, G. Kokotos, E. Papavassilopoulou, C. Potamitis, C. Photakis, P. Chatzigeorgiou, K. Viras, C. Koukoulitsa, E. Kalatzis, S. Durdagi, in *Essays on Contemporary Peptide Science* (Ed: P. Cordopatis), vol. *6*, Research Signpost, India, **2011** p, 95–112.
[40] H. Brötz, G. Bierbaum, K. Leopold, P. E. Reynolds, H. -G. Sahl, *Antimicrob. Agents Chemoter.* **1998**, *42*, 154.
[41] V. Arjunan, S. Subramanian, S. Mohan, *Spectrochim. Acta, Part A* **2001**, *57*, 2547.
[42] M. X-Bradley, Application Note: 50733, Thermo Electron Scientific Instruments LLC, Madison, WI, **2007**.
[43] M. J. Frisch, G. W. Trucks, H. B. Schlegel, G. E. Scuseria, M. A. Robb, J. R. Cheeseman, J. A. Montgomery, Jr., T. Vreven, K. N. Kudin, J. C. Burant, J. M. Millam, S. S. Iyengar, J. Tomasi, V. Barone, B. Mennucci, M. Cossi, G. Scalmani, N. Rega, G. A. Petersson, H. Nakatsuji, M. Hada, M. Ehara, K. Toyota, R. Fukuda, J. Hasegawa, M. Ishida, T. Nakajima, Y. Honda, O. Kitao, H. Nakai, M. Klene, X. Li, J. E. Knox, H. P. Hratchian, J. B. Cross, V. Bakken, C. Adamo, J. Jaramillo, R. Gomperts, R. E. Stratmann, O. Yazyev, A. J. Austin, R. Cammi, C. Pomelli, J. W. Ochterski, P. Y. Ayala, K. Morokuma, G. A. Voth, P. Salvador, J. J. Dannenberg, V. G. Zakrzewski, S. Dapprich, A. D. Daniels, M. C. Strain, O. Farkas, D. K. Malick, A. D. Rabuck, K. Raghavachari, J. B. Foresman, J. V. Ortiz, Q. Cui, A. G. Baboul, S. Clifford, J. Cioslowski, B. B. Stefanov, G. Liu, A. Liashenko, P. Piskorz, I. Komaromi, R. L. Martin, D. J. Fox, T. Keith, M. A. Al-Laham, C. Y. Peng, A. Nanayakkara, M. Challacombe, P. M. W. Gill, B. Johnson, W. Chen, M. W. Wong, C. Gonzalez, J. A. Pople, Revision E.01, Gaussian, Inc., Wallingford CT, **2003**
[44] C. Lee, W. Yang, R. G. Parr, *Phys. Rev. B: Condens. Matter Mater. Phys.* **1988**, *37*, 785.
[45] A. D. Becke, *J. Chem. Phys.* **1993**, *98*, 5648.
[46] P. J. Stephens, F. J. Devlin, C. F. Chabalowski, M. J. Frisch, *J. Phys. Chem.* **1994**, *98*, 11623.
[47] T. Clark, J. Chandrasekhar, G. W. Spitznagel, P. V. R. Schleyer, *J. Comp. Chem.* **1983**, *4*, 294.
[48] G. A. Petersson, M. A. Al-Laham, *J. Chem. Phys.* **1991**, *94*, 6081.
[49] R. Dennington, T. Keith, J. Millam, Semichem Inc., Shawnee Mission KS, **2009**.
[50] Y. -P. Zhang, R. N. A. H. Lewis, R. N. McElhaney, *Biophys. J.* **1997**, *72*, 779.
[51] D. A. Pink, T. J. Green, D. Chapman, *Biochemistry* **1981**, *20*, 6692.
[52] X. -M. Li, B. Zhao, D. -Q. Zhao, J. -Z. Ni, Y. Wu, W. -Q. Xu, *Thin Solid Films* **1996**, *284*, 762.
[53] S. Bonora, A. Torreggiani, G. Fini, *Thermochim. Acta* **2003**, *408*, 55.
[54] S. L. Wunder, S. Ahmed, Z. S. Nickolov, Spectroscopy, **2011.**
[55] B. Ewen, G. R. Strobl, D. Richter, *Faraday Discuss. Chem. Soc.* **1980**, *69*, 19.
[56] 56. M. Maroncelli, S. P. Qi, H. L. Strauss, R. G. Snyder, *J. Am. Chem. Soc.* **1982**, *104*, 6237.
[57] R. G. Snyder, M. Maroncelli, H. L. Strauss, C. A. Elliger, D. G. Cameron, H. L. Casal, H. H. Mantsch, *J. Am. Chem. Soc.* **1983**, *105*, 133.
[58] D. L. Dorset, B. Moss, J. C. Wittmannt, B. Lotz, *Proc. Natl. Acad. Sci. U. S. A.* **1984**, *81*, 1913.
[59] E. Bicknell-Brown, K. Brown, W. B. Person, *J. Raman Spectrosc.* **1982**, *12*, 180.
[60] D. E. Elmore, *FEBS Lett.* **2006**, *580*, 144.
[61] W. Zhao, T. Róg, A. A. Gurtovenko, I. Vattulainen, M. Karttunen, *Biophys. J.* **2007**, *92*, 1114.
[62] J. Pimthon, R. Willumeit, A. Lendlein, D. Hofmann, *J. Mol. Struct.* **2009**, *921*, 38.
[63] E. Bicknell-Brown, K. G. Brown, *Biochem. Biophys. Res. Commun.* **1980**, *94*, 638.
[64] E. Bicknell-Brown, K. Brown, W. B. Person, *J. Am. Chem. Soc.* **1980**, *102*, 5486.
[65] I. W. Levin, E. Mushayakarara, R. Bittman, *J. Raman Spectrosc.* **1982**, *13*, 231.
[66] R. N. H. Lewis, R. N. McElhaney, W. Pohle, H. H. Mantsch, *Biophys. J.* **1994**, *67*, 2367.